

**Cytotoxic mixed-ligand copper(II) complexes with 1H-tetrazole-5-acetic acid and oligopyridine derivatives**

Ekaterina A. Ermakova, Yuliya A. Golubeva, Ksenia S. Smirnova, Lyubov S. Klyushova, Alexey S. Berezin, Leonid N. Fetisov, Alexandra E. Svyatogorova, Natalia O. Andros, Alexander A. Zubenko, Elizaveta V. Lider\*

**Supplementary material**

Two types of single crystals have been isolated from the mother liquor of a mixed-ligand copper(II) complex with 1,10-phenanthroline, namely blue blocks and light blue plates. Both of complexes are polymeric structures, but crystallize in different space groups –  $C2/c$  and  $P2_1/c$ . The first compound  $[\text{Cu}_3(\text{phen})_2(\text{H}_2\text{O})(\text{HL})_2\text{L}_2]_n \cdot 6n\text{H}_2\text{O}$  (**4a**) has two crystallography non-equivalent copper(II) ions in slightly distorted square pyramidal environment (Fig. S1a). The latter one can be confirmed by  $\tau_5$ -parameter [A. W. Addison, T. N. Rao, J. Reedijk, J. Van Rijn and G. C. Verschoor, *J. Chem. Soc. Dalt. Trans.*, 1984, 1349–1356], as well as continuous shape measures  $S(C4v)$  indicating the resembles the obtained polyhedron with an ideal one [SHAPE 2.1 program for the stereochemical analysis of molecular fragments by means of continuous shape measures and associated tools]. For Cu1 ion,  $\tau_5$ -parameter and  $S(C4v)$  are equal to 0.10 and 0.62 respectively, for Cu2 – 0.41 and 1.06. The Cu1 ion is surrounded by two nitrogen atoms of phen, nitrogen and oxygen atoms of tetrazolate, as well as nitrogen atom of another  $\text{HL}^-$  (Fig. S1a). As for the second copper(II) ion, four nitrogen atoms of four tetrazole ligands and the oxygen atom of water molecule are coordinated to the central atom. As it can be seen in Figure S1a, the unit  $[\text{Cu}_3(\text{phen})_2(\text{H}_2\text{O})(\text{HL})_2\text{L}_2]$  contains both fully deprotonated  $\text{L}^{2-}$  molecule and ligand  $\text{HL}^-$  with non-deprotonated carboxyl group. As a result, tetrazolate ligand exhibits various coordination modes, such as protonated molecule demonstrates bidentate-bridging coordination mode via N1 and N4 atoms of tetrazolate ring. The deprotonated  $\text{L}^{2-}$  ligand chelates the Cu1 ion by N1 atom of tetrazole and carboxylate O atom, as well as N4 atom is coordinated to Cu2 ion, thereby  $\text{L}^{2-}$  also serves as bridge between two neighboring metal ions. The bridging coordination results in the formation of rhombus-type polymer chain, arranging along  $c$ -axis of unit cell (Fig. S1b). These polymer chains are packing in layered structure due to the presence of  $\pi$ -stacking between neighboring phen molecules (3.580 Å). This two-dimensional structure is arranged parallel to  $ac$  crystallographic plane (Fig. S8). In addition, this compound contains non-coordinated water molecules.

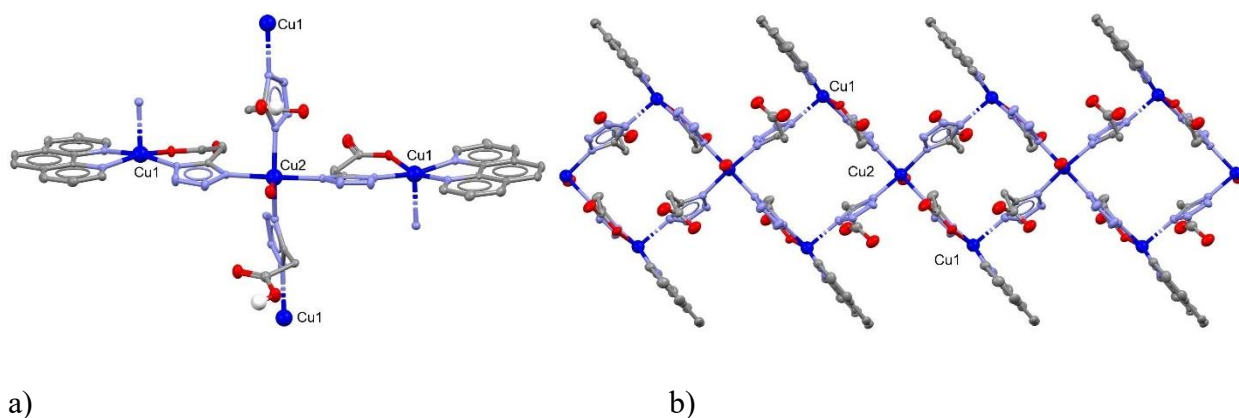


Figure S1. The coordination nodes of copper(II) ions in complex  $[\text{Cu}_3(\text{phen})_2(\text{H}_2\text{O})(\text{HL})_2\text{L}_2]_n \cdot 6n\text{H}_2\text{O}$  (a) and rhombus-type polymer chain (b). Hydrogen atoms and water molecules are not shown.

The second structure turned out to be mononuclear compound  $[\text{Cu}(\text{bipy})(\text{H}_2\text{O})\text{L}]$  (**6a**), where bipy and  $\text{L}^{2-}$  demonstrate bidentate-cycling coordination (Fig. S2). The coordination sphere of copper(II) ion is completed by water molecule to square pyramid ( $S(C4v) = 1.02$ ,  $\tau_5 = 0.16$ ).

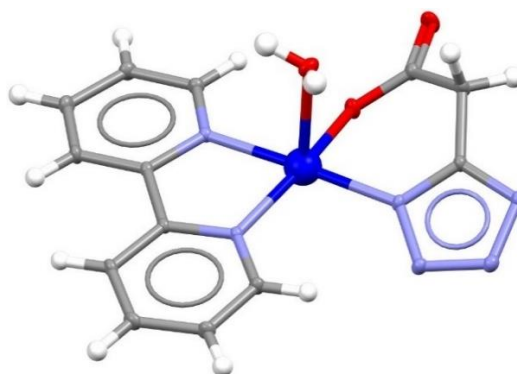


Figure S2. The structure of  $[\text{Cu}(\text{bipy})(\text{H}_2\text{O})\text{L}]$ .

In case of copper(II) complex with 4,4'-dimethylbipyridine, it have been managed to distinguish three types of single crystals with different structures, namely  $[\text{Cu}(\text{dmbipy})(\text{HL})_2]$  (**5a**),  $[\text{Cu}_3(\text{dmpiby})_2(\text{HL})_2\text{L}_2]_n \cdot 2n\text{H}_2\text{O} \cdot 2nC_2H_5OH$  (**5b**) and  $[\text{Cu}(\text{dmbipy})\text{L}]_n$  (**5**). The first compound  $[\text{Cu}_3(\text{dmpiby})_2(\text{HL})_2\text{L}_2]_n \cdot 2n\text{H}_2\text{O} \cdot 2nC_2H_5OH$  (blue plates) is rhombus-type polymer chain similar to previously described  $[\text{Cu}_3(\text{phen})_2(\text{H}_2\text{O})(\text{HL})_2\text{L}_2]_n \cdot 6n\text{H}_2\text{O}$ . The unit  $[\text{Cu}_3(\text{dmpiby})_2(\text{HL})_2\text{L}_2]_n$  also contains as fully deprotonated  $\text{L}^{2-}$  molecule and ligand  $\text{HL}^-$  with non-deprotonated carboxyl group (Fig. S3a). There are two crystallography non-equivalent copper(II) ions with different coordination polyhedron: square pyramid is observed for Cu1 ( $S(C4v)=1.02$ ,  $\tau_5=0.065$ ) and octahedron ( $S(Oh)=1.48$ ) – for Cu2. As in mixed-ligand complex with phen, two nitrogen atoms of dmbipy, nitrogen and oxygen atoms of  $\text{L}^{2-}$ , as well as nitrogen atom of another anion  $\text{HL}^-$  are

coordinated to Cu1 (Fig. S3a). Octahedral environment of Cu2 consists of nitrogen and oxygen atoms of two anion  $HL^-$  (chelating coordination), and also two nitrogen atoms of two  $L^{2-}$ . Thus, both anions  $L^{2-}$  and  $HL^-$  exhibit bidentate-bridging coordination, which results in rhombus-type polymer chain, arranging along *b*-axis of unit cell (Fig. S3b). Due to the presence of 4,4'-dimethylbipyridine,  $\pi$ - $\pi$  interaction (3.935 Å) between neighboring dmbipy molecules is observed leading to two-dimensional structure, which is parallel to *bc* crystallographic plane (Fig. S10). The obtained compound also contains non-coordinated water and ethanol molecules.

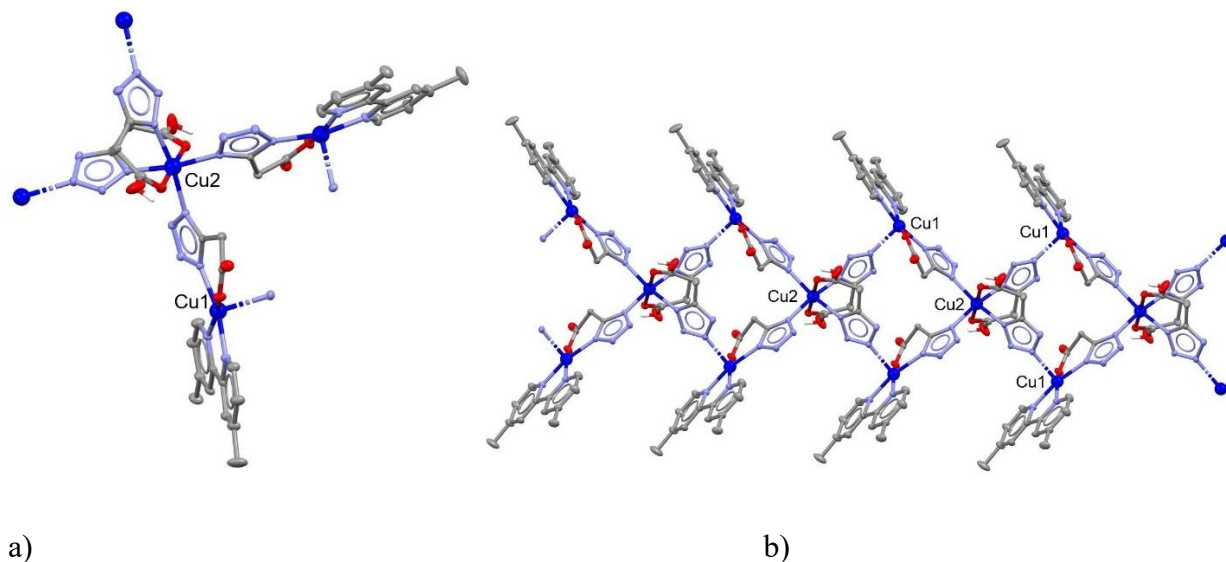


Figure S3. The coordination nodes of copper(II) ions in complex  $[Cu_3(dmbipy)_2(HL)_2L_2]_n \cdot 2nH_2O \cdot 2nC_2H_5OH$  (a) and rhombus-type polymer chain (b). Hydrogen atoms and water molecules are not shown.

According to single-crystal XRD-analysis, light-blue blocks turn out mononuclear compound  $[Cu(dmbipy)(HL)_2]$  (Fig. S4). The square pyramidal environment ( $S(C4v)=0.76$ ,  $\tau_5=0.18$ ) of copper(II) ion consists of two nitrogen atoms of dmbipy molecule (chelating coordination), nitrogen and oxygen atoms of one deprotonated  $HL^-$  anion (chelating coordination) and nitrogen atom of another  $HL^-$  – monodentate coordination (Fig. S4). The neighboring mononuclear compounds are packed as chains due to  $\pi$ -stacking between tetrazole and pyridine cycles (3.569 Å), as well as C-H $\cdots$ N contacts (Fig. S11).

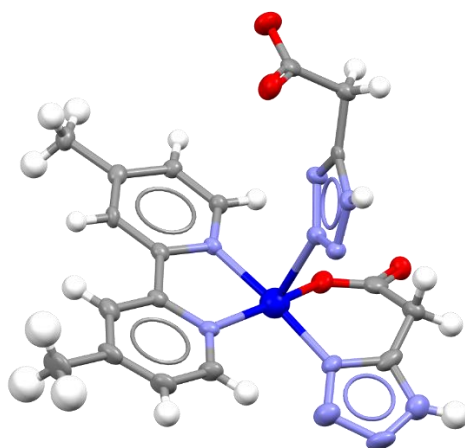


Figure S4. The structure of mononuclear compound  $[\text{Cu}(\text{dmbipy})(\text{HL})_2]$ .

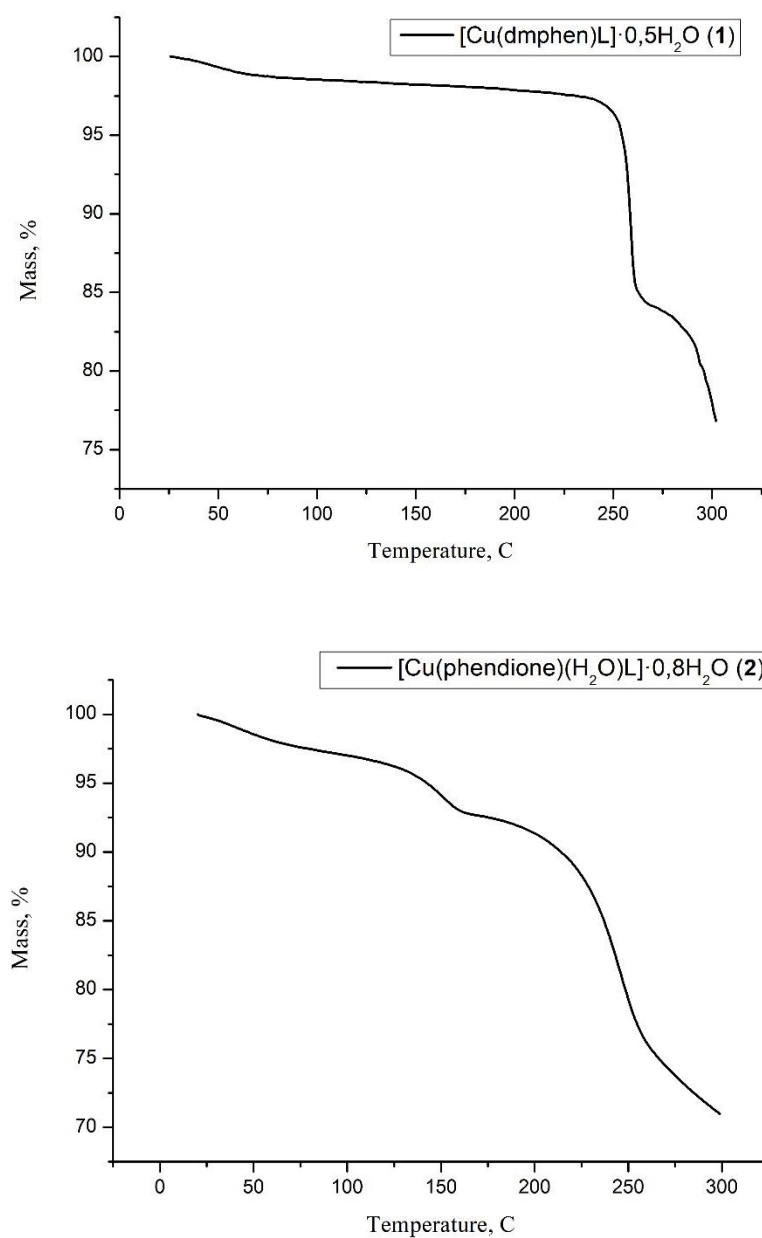
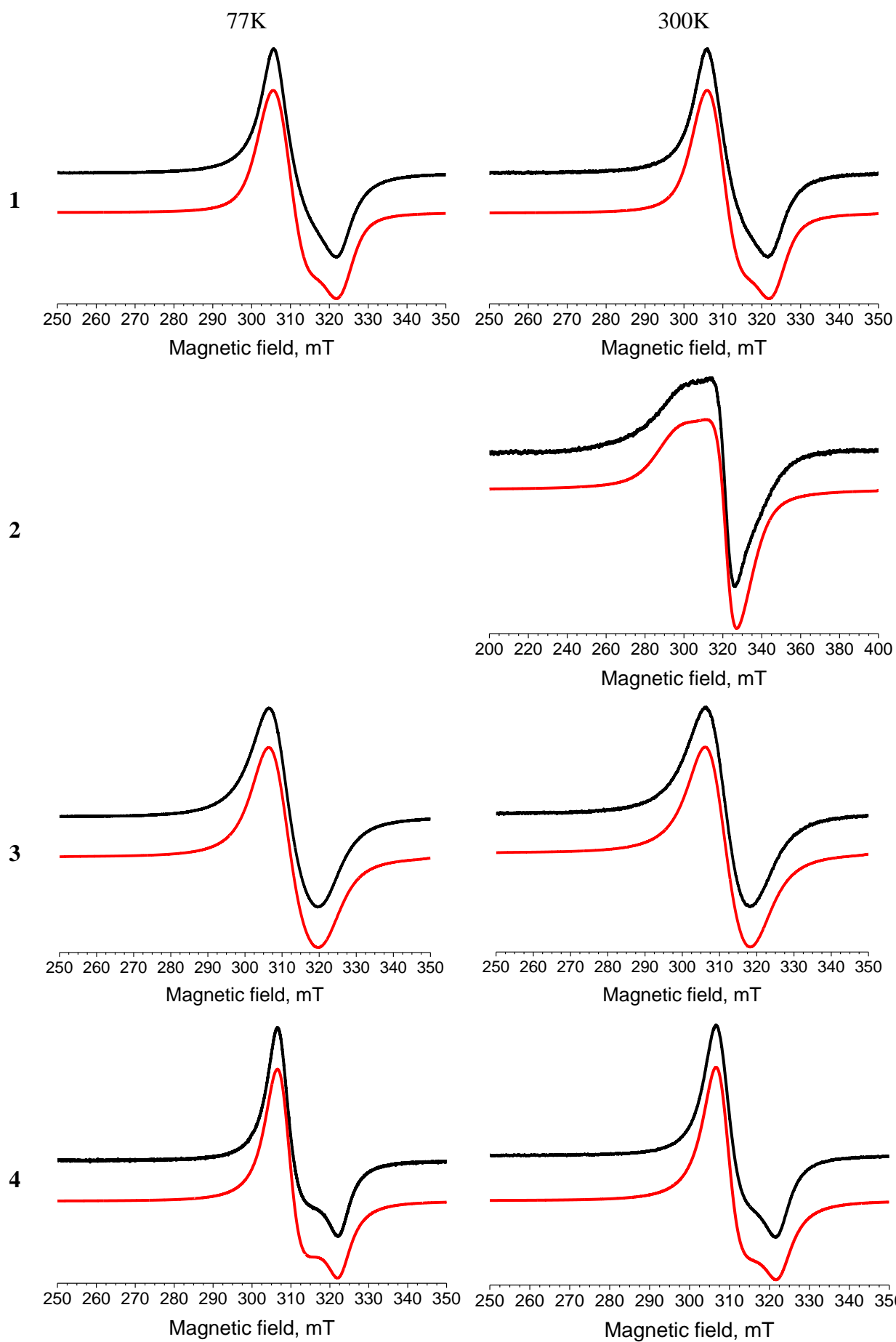


Fig S5. TGA for complexes **1**, **2**.



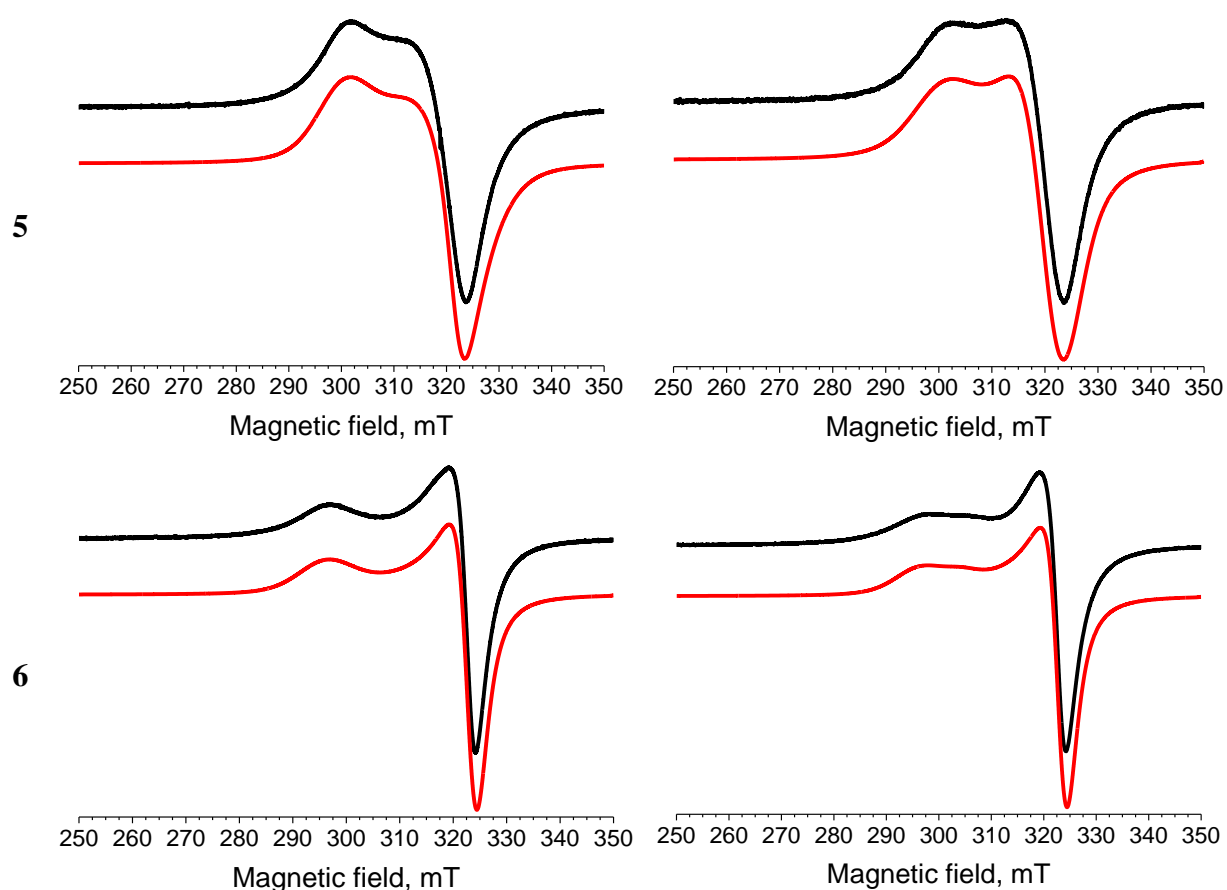
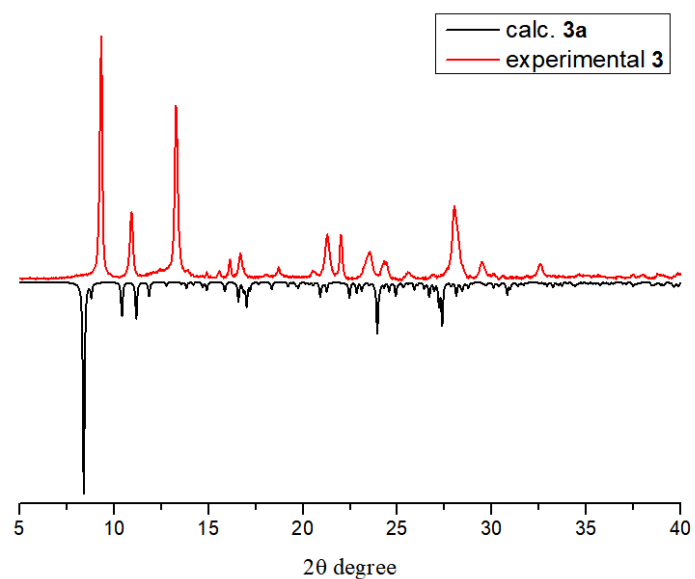


Figure S6. X-band EPR spectra of complexes **1-6**, where black is experimental, red is simulated. The experiments were carried out at 77K and 300 K.



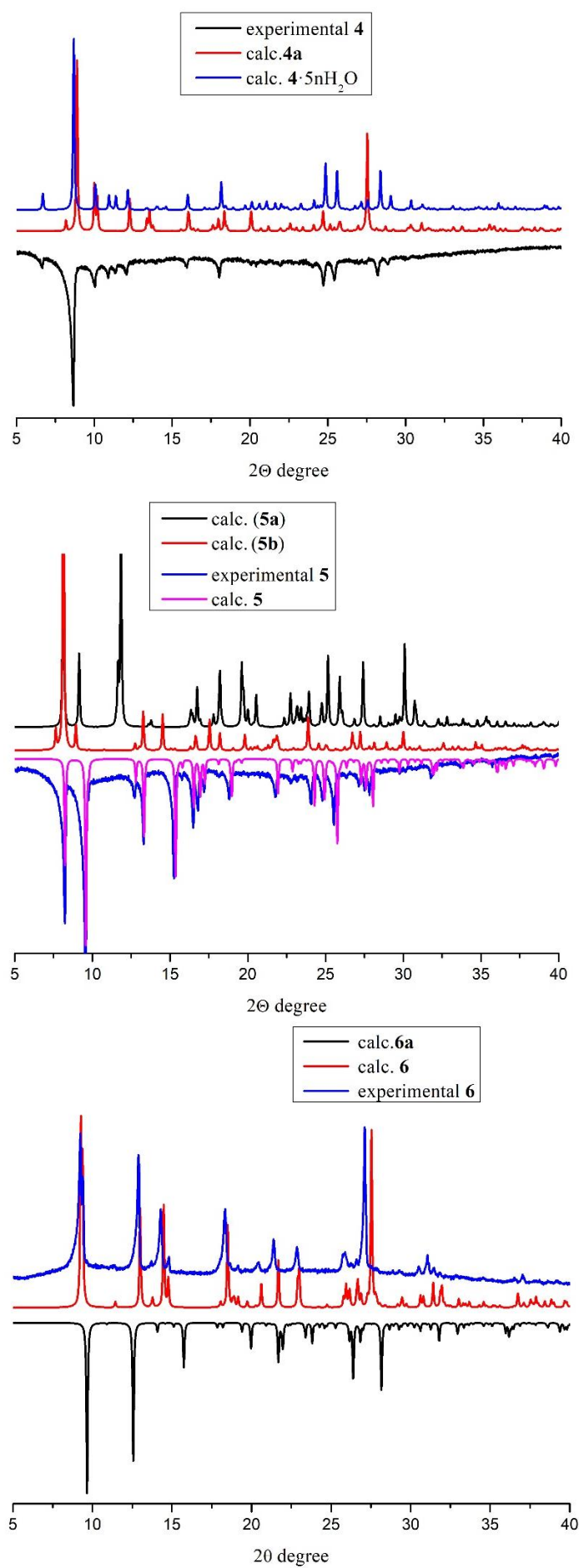


Fig S7. X-ray powder patterns for complexes **3-6**.



Table S1. Crystallographic data and details of structure refinement for the copper(II) compounds.

Compound	<b>3a</b>	<b>4</b>	<b>4a</b>	<b>5</b>	<b>5a</b>	<b>5b</b>	<b>6</b>	<b>6a</b>
Empirical formula	C <sub>32</sub> H <sub>30</sub> Cl <sub>2</sub> Cu <sub>2</sub> N <sub>12</sub> O <sub>8</sub> S	C <sub>15</sub> H <sub>15</sub> CuN <sub>6</sub> O <sub>4.5</sub>	C <sub>36</sub> H <sub>36</sub> Cu <sub>3</sub> N <sub>20</sub> O <sub>15</sub>	C <sub>15</sub> H <sub>14</sub> CuN <sub>6</sub> O <sub>2</sub>	C <sub>18</sub> H <sub>18</sub> CuN <sub>10</sub> O <sub>4</sub>	C <sub>40</sub> H <sub>48</sub> Cu <sub>3</sub> N <sub>20</sub> O <sub>12</sub>	C <sub>13</sub> H <sub>10</sub> CuN <sub>6</sub> O <sub>2</sub>	C <sub>13</sub> H <sub>12</sub> CuN <sub>6</sub> O <sub>3</sub>
Formula weight	940.72	414.87	1179.43	373.86	501.96	1193.60	345.81	363.83
Crystal system	monoclinic	monoclinic	monoclinic	monoclinic	monoclinic	monoclinic	orthorhombic	triclinic
Space group	P2 <sub>1</sub> /c	P2 <sub>1</sub> /c	C2/c	P2 <sub>1</sub> /c	P2 <sub>1</sub> /c	P2/n	Pbca	P-1
a/Å	19.0581(7)	9.1842(2)	12.9458(4)	11.1628(6)	11.5059(5)	13.6079(4)	8.6431(2)	7.3702(2)
b/Å	9.1854(4)	17.3175(5)	19.8921(6)	18.0968(10)	21.8114(9)	9.0225(2)	16.2056(3)	10.2412(2)
c/Å	21.4525(9)	20.4838(7)	17.8258(5)	7.7861(4)	8.6454(4)	19.8301(5)	18.2899(4)	10.3398(3)
α/°	90	90	90	90	90	90	90	71.3900(10)
β/°	101.2310(10)	96.1010(10)	96.840(1)	106.210(2)	110.5490(10)	93.8720(10)	90	70.1300(10)
γ/°	90	90	90	90	90	90	90	73.8830(10)
Volume/Å <sup>3</sup>	3683.5(3)	3239.44(16)	4557.8(2)	1510.35(14)	2031.60(15)	2429.13(11)	2561.80(9)	682.97(3)
Z	4	4	4	4	4	2	8	2
ρ <sub>calc</sub> /cm <sup>3</sup>	1.696	1.701	1.672	1.644	1.641	1.629	1.793	1.769
μ/mm <sup>-1</sup>	1.426	1.389	1.474	1.468	1.127	1.384	1.723	1.626
Crystal size/mm <sup>3</sup>	0.08 × 0.06 × 0.03	0.15 × 0.1 × 0.01	0.1 × 0.05 × 0.03	0.14 × 0.09 × 0.05	0.1 × 0.05 × 0.03	0.14 × 0.1 × 0.04	0.2 × 0.08 × 0.04	0.15 × 0.15 × 0.04
2θ range for data collection/°	4.06 to 56.65	4.00 to 56.59	3.77 to 51.38	4.42 to 54.25	3.78 to 51.37	4.12 to 61.02	4.45 to 69.96	4.27 to 66.44
Index ranges	-16 ≤ h ≤ 25, -12 ≤ k ≤ 12, -28 ≤ l ≤ 28	-11 ≤ h ≤ 12, -23 ≤ k ≤ 19, -27 ≤ l ≤ 25	-15 ≤ h ≤ 15, -24 ≤ k ≤ 24, -21 ≤ l ≤ 21	-13 ≤ h ≤ 14, -23 ≤ k ≤ 23, -9 ≤ l ≤ 9	-14 ≤ h ≤ 14, -26 ≤ k ≤ 26, -10 ≤ l ≤ 10	-19 ≤ h ≤ 16, -12 ≤ k ≤ 12, -28 ≤ l ≤ 28	-13 ≤ h ≤ 13, -26 ≤ k ≤ 26, -29 ≤ l ≤ 29	-11 ≤ h ≤ 11, -14 ≤ k ≤ 15, -15 ≤ l ≤ 15
Reflections collected	50153	19262	21633	16480	20793	31733	37498	14229
Independent reflections	9177 [R <sub>int</sub> = 0.0626, R <sub>sigma</sub> = 0.0675]	8000 [R <sub>int</sub> = 0.0476, R <sub>sigma</sub> = 0.0701]	4347 [R <sub>int</sub> = 0.0725, R <sub>sigma</sub> = 0.0579]	3319 [R <sub>int</sub> = 0.0517, R <sub>sigma</sub> = 0.0405]	3856 [R <sub>int</sub> = 0.0960, R <sub>sigma</sub> = 0.0761]	7411 [R <sub>int</sub> = 0.0483, R <sub>sigma</sub> = 0.0445]	5634 [R <sub>int</sub> = 0.0645, R <sub>sigma</sub> = 0.0405]	5222 [R <sub>int</sub> = 0.0347, R <sub>sigma</sub> = 0.0408]
Restraints/parameters	0/525	0/493	2/351	0/219	0/300	2/333	0/199	0/209
GooF on F <sup>2</sup>	1.156	1.034	1.056	1.043	1.040	1.049	1.161	0.852
Final R indexes [I>=2σ (I)]	R <sub>1</sub> = 0.0899, wR <sub>2</sub> = 0.1948	R <sub>1</sub> = 0.0475, wR <sub>2</sub> = 0.0991	R <sub>1</sub> = 0.0471, wR <sub>2</sub> = 0.1151	R <sub>1</sub> = 0.0411, wR <sub>2</sub> = 0.0847	R <sub>1</sub> = 0.0604, wR <sub>2</sub> = 0.1285	R <sub>1</sub> = 0.0542, wR <sub>2</sub> = 0.1469	R <sub>1</sub> = 0.0929, wR <sub>2</sub> = 0.1870	R <sub>1</sub> = 0.0340, wR <sub>2</sub> = 0.0840
Final R indexes [all data]	R <sub>1</sub> = 0.1192, wR <sub>2</sub> = 0.2078	R <sub>1</sub> = 0.0747, wR <sub>2</sub> = 0.1120	R <sub>1</sub> = 0.0733, wR <sub>2</sub> = 0.1287	R <sub>1</sub> = 0.0524, wR <sub>2</sub> = 0.0890	R <sub>1</sub> = 0.0978, wR <sub>2</sub> = 0.1435	R <sub>1</sub> = 0.00763, wR <sub>2</sub> = 0.1642	R <sub>1</sub> = 0.1067, wR <sub>2</sub> = 0.1933	R <sub>1</sub> = 0.0403, wR <sub>2</sub> = 0.0894
Largest diff. peak / hole / e, Å <sup>-3</sup>	2.34/-1.30	0.50/-0.69	0.75/-0.52	0.44/-0.45	1.17/-0.48	1.92/-0.90	2.48/-1.45	0.67/-0.40
CCDC number	2223376	2221803	2221804	2221807	2221806	2221808	2221809	2221805

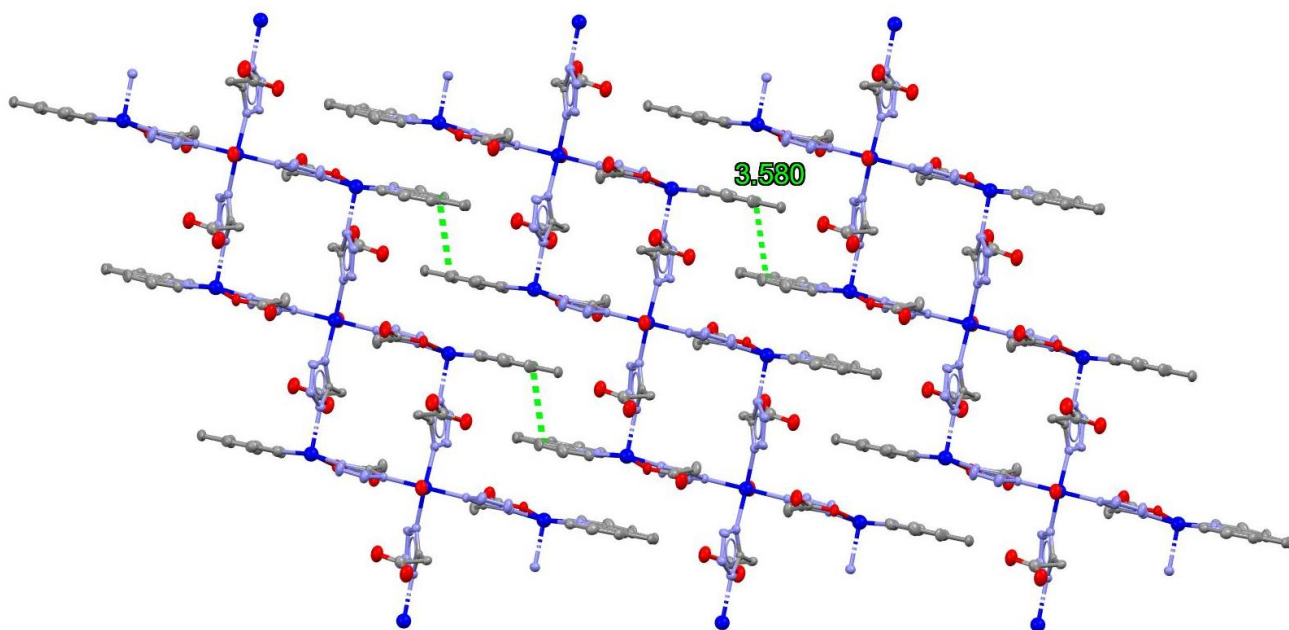


Figure S8. The layered structure of  $[\text{Cu}_3(\text{phen})_2(\text{H}_2\text{O})(\text{HL})_2\text{L}_2]_n \cdot 6\text{H}_2\text{O}$  (**4a**) is due to  $\pi$ -stacking. Hydrogen atoms and water molecules are not shown.

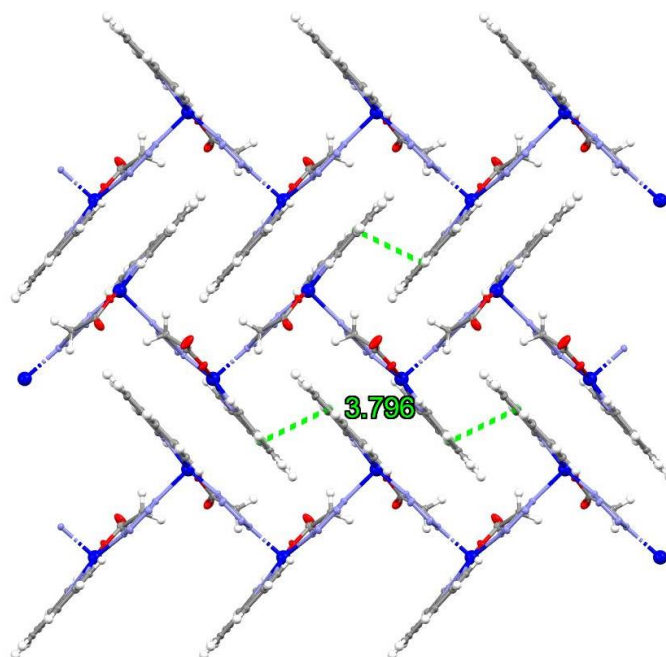


Figure S9. The layered structure of  $[\text{Cu}(\text{phen})\text{L}]_n \cdot 2.5n\text{H}_2\text{O}$  (**4**) is due to  $\pi$ -stacking. Water molecules are not shown.

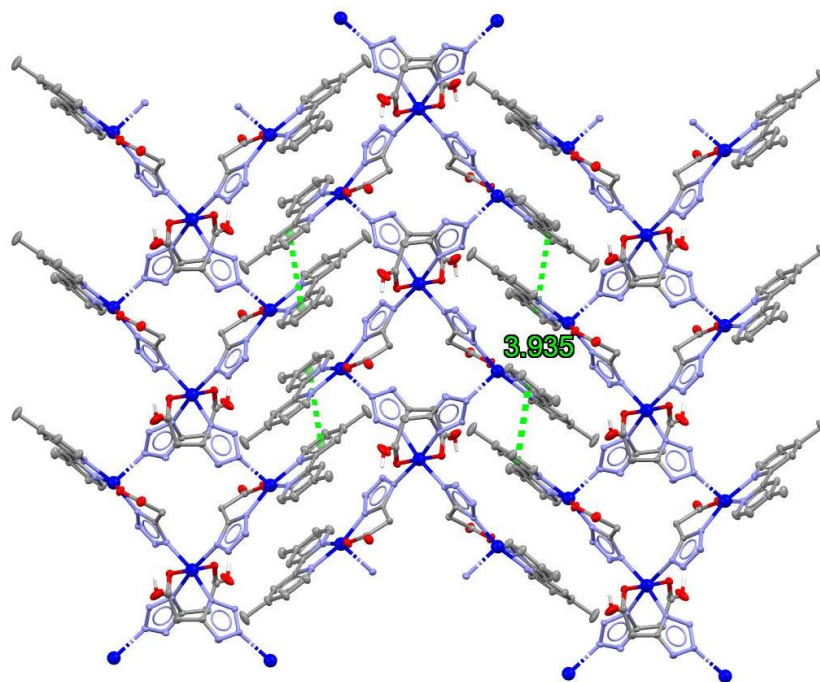


Figure S10. The layered structure of  $[\text{Cu}_3(\text{dmpiby})_2(\text{HL})_2\text{L}_2]_n \cdot 2n\text{H}_2\text{O} \cdot 2n\text{C}_2\text{H}_5\text{OH}$  (**5b**) is due to  $\pi$ -stacking. Hydrogen atoms and water molecules are not shown.

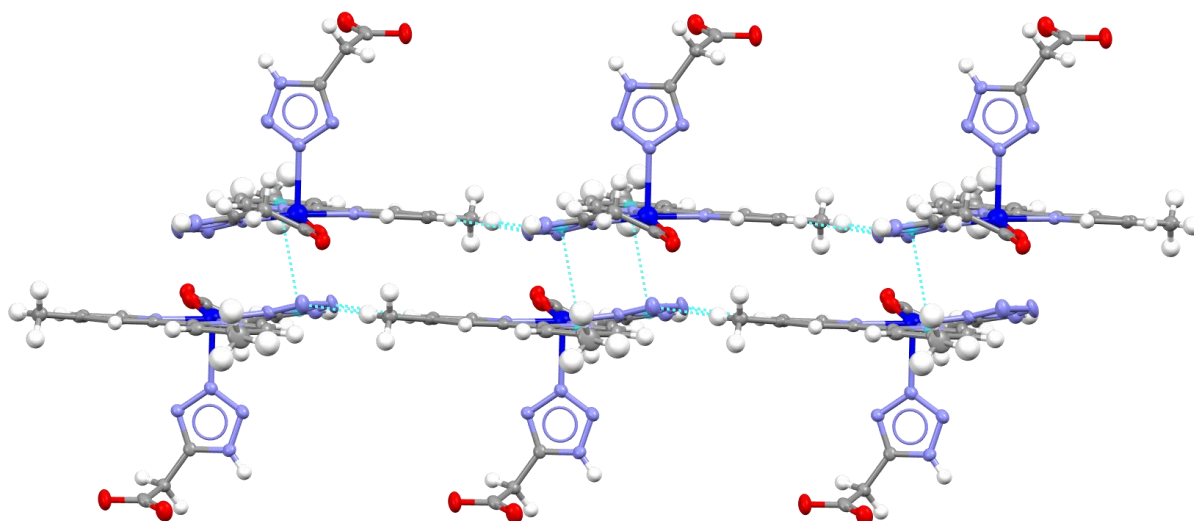


Figure S11. The packing of mononuclear compound  $[\text{Cu}(\text{dmbipy})(\text{HL})_2]$  (**5a**) due to  $\pi$ -stacking and C-H $\cdots$ N contacts.

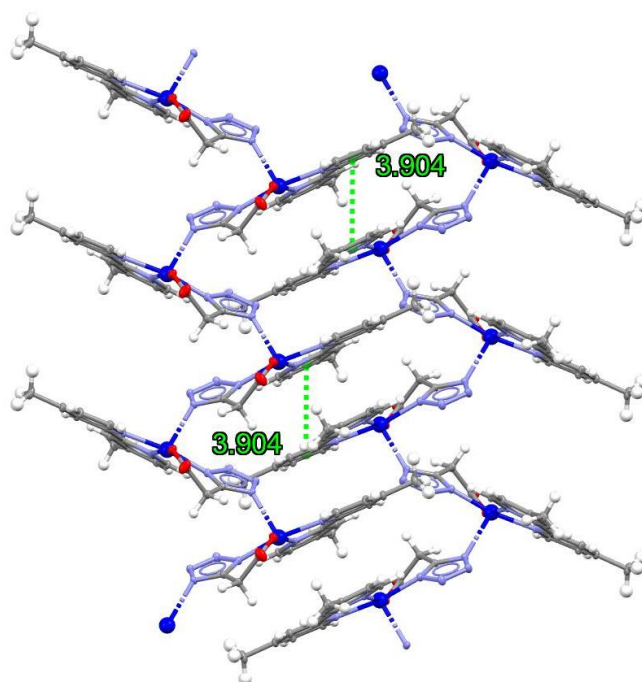


Figure S12. The layered structure of  $[\text{Cu}(\text{dmbipy})\text{L}]_n$  (**5**) is due to  $\pi$ -stacking.

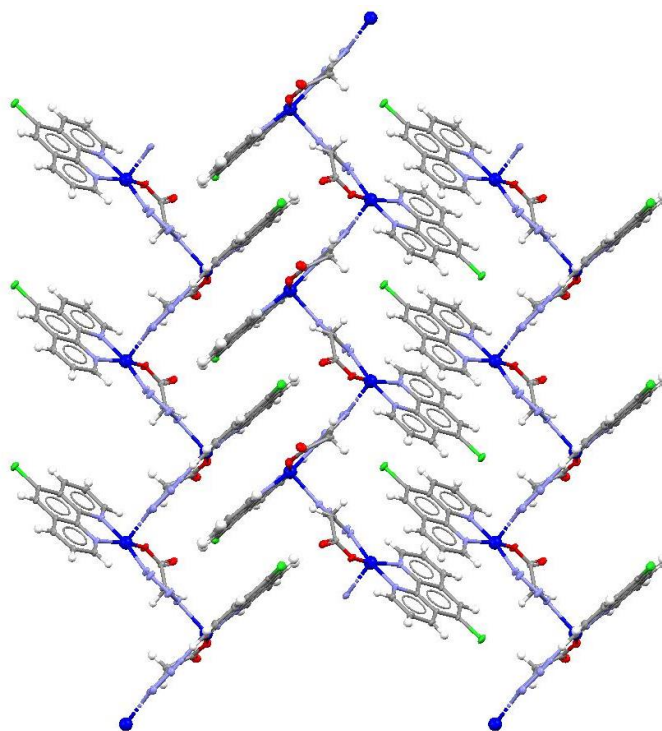
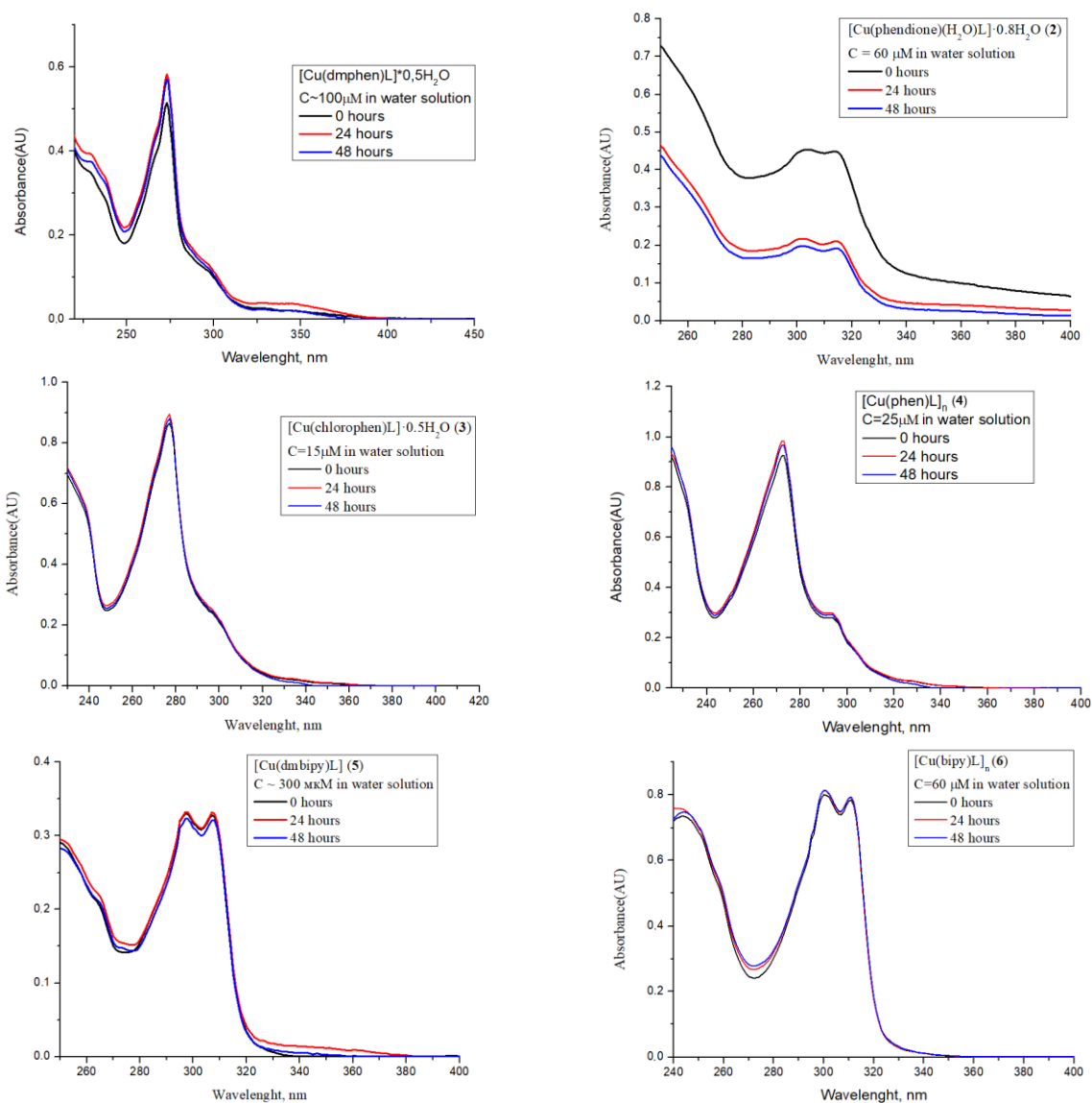
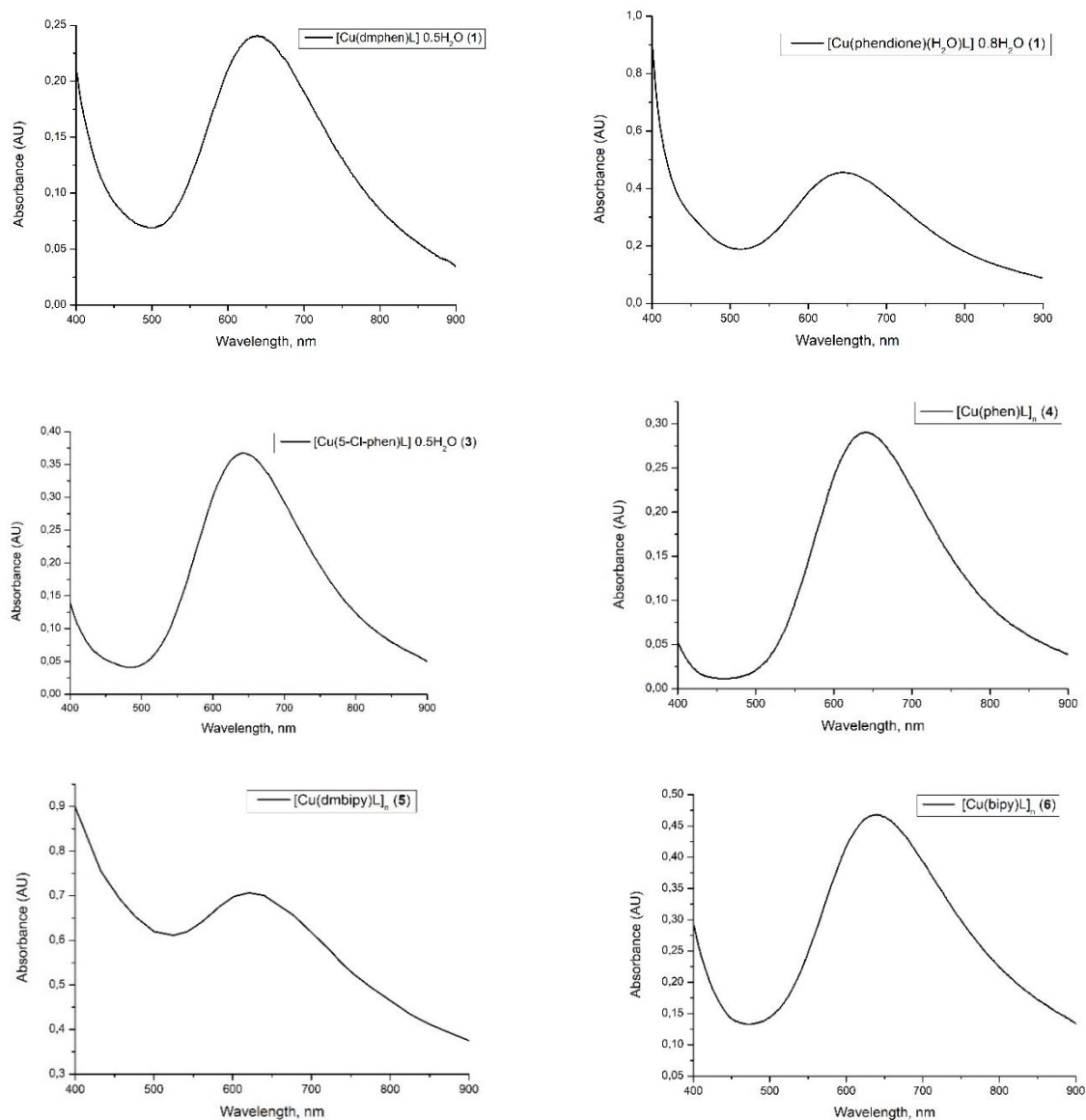


Figure S13. The layered structure of  $[\text{Cu}(5\text{-Cl-phen})\text{L}]_n \cdot 0.5n\text{DMSO} \cdot 1.5n\text{H}_2\text{O}$  (**3a**) is due to  $\pi$ -stacking. Solvent molecules are not shown.



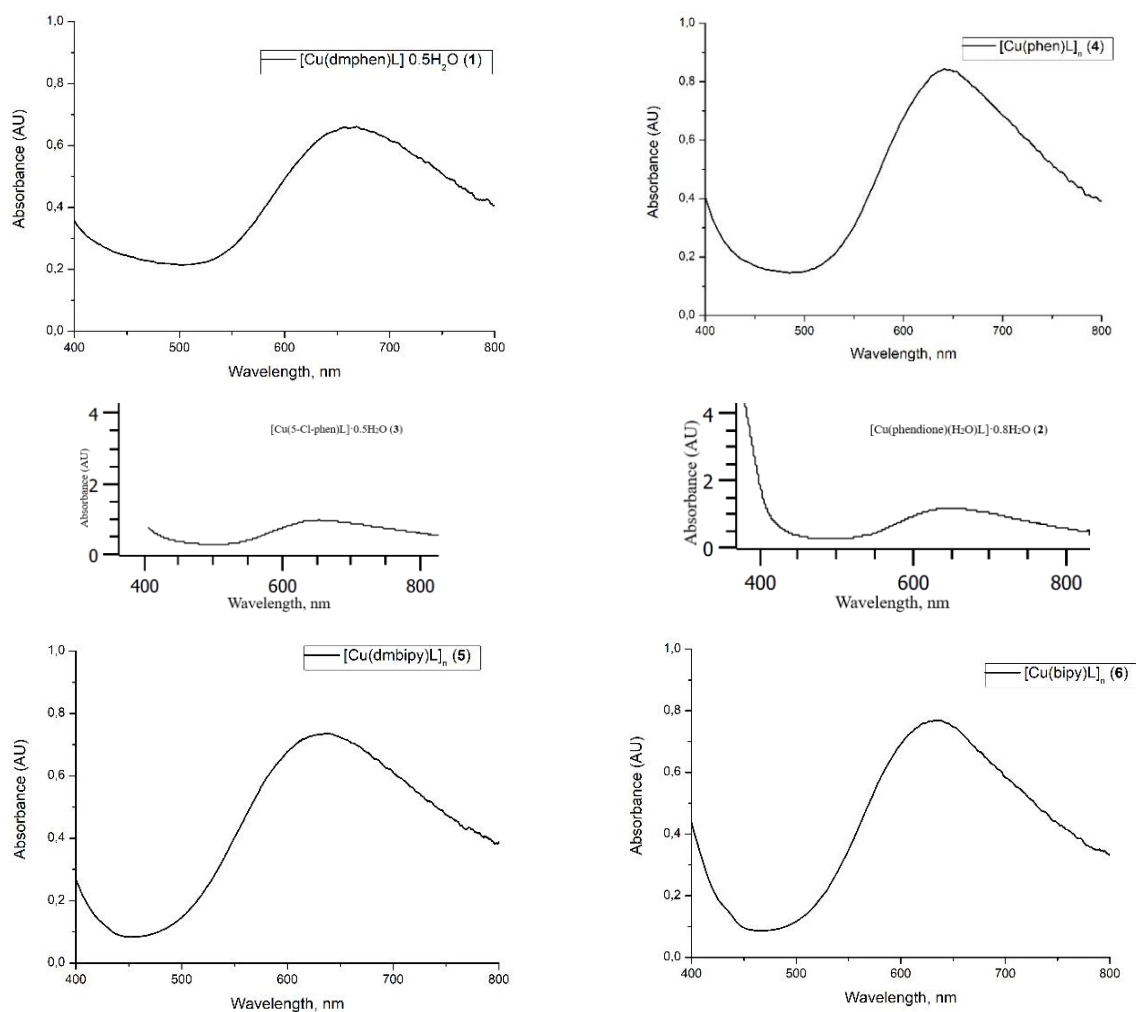
a)

Fig.S14. a) Time-dependent UV absorption spectra of complexes **1-6** in aqueous solution at  $t = 0$ , 24, 48 h; b) Visible absorption spectra of the obtained complexes in DMSO (**1**, **2**, **5**, **6**) or EtOH (**3**, **4**) solution; c) diffuse reflectance spectra of the complexes **1-6**.



b)

Fig.S14. a) Time-dependent UV absorption spectra of complexes **1-6** in aqueous solution at  $t = 0, 24, 48$  h; b) Visible absorption spectra of the obtained complexes in DMSO (**1, 2, 5, 6**) or EtOH (**3, 4**) solution; c) diffuse reflectance spectra of the complexes **1-6**.



c)

Fig.S14. a) Time-dependent UV absorption spectra of complexes **1-6** in aqueous solution at  $t = 0$ , 24, 48 h; b) Visible absorption spectra of the obtained complexes in DMSO (**1, 2, 5, 6**) or EtOH (**3, 4**) solution; c) diffuse reflectance spectra of the complexes **1-6**.

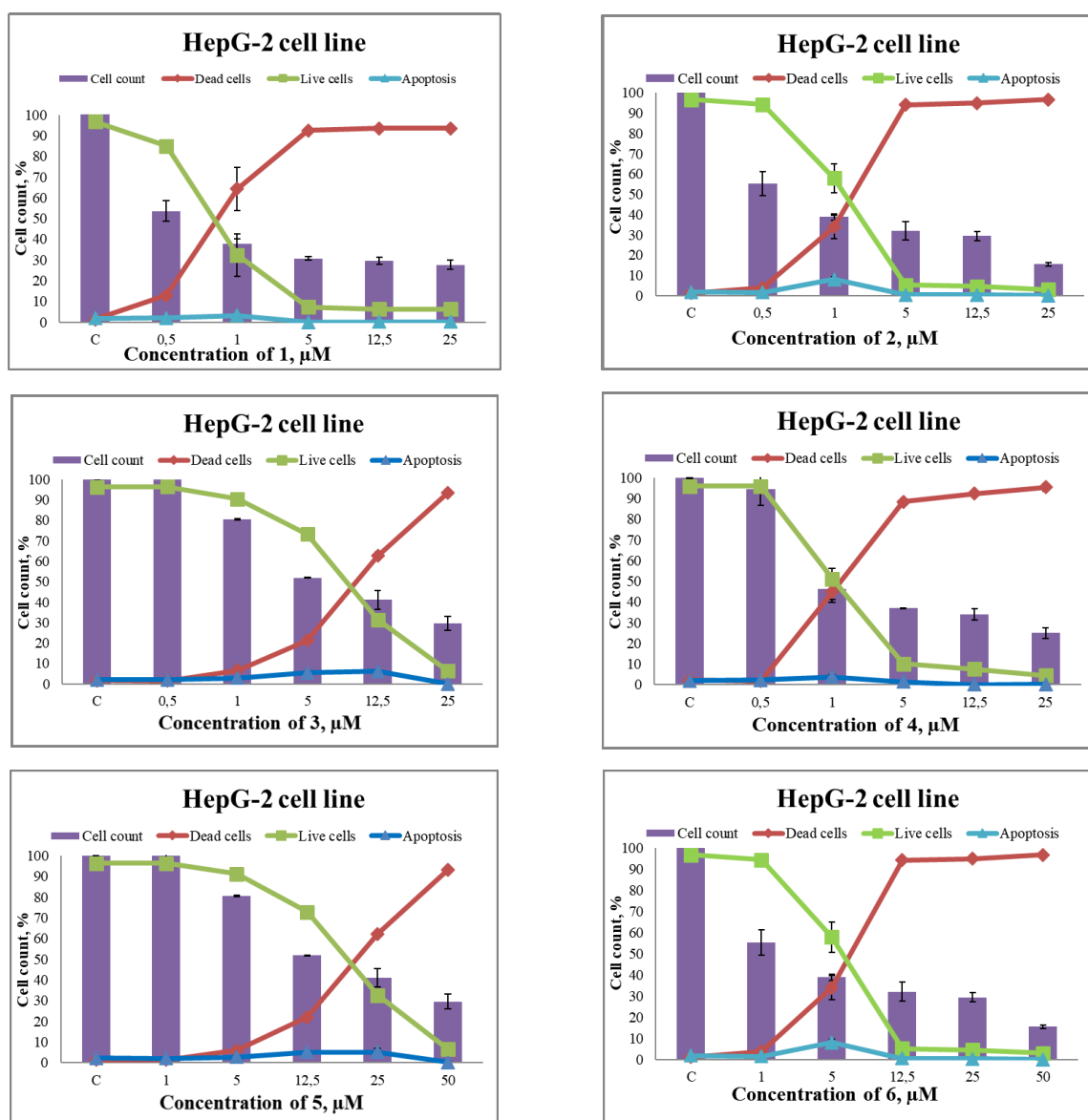


Figure S15. Effect of the copper(II) complexes on the viability of HepG-2 cells determined by dual staining with Hoechst 33342/propidium iodide.



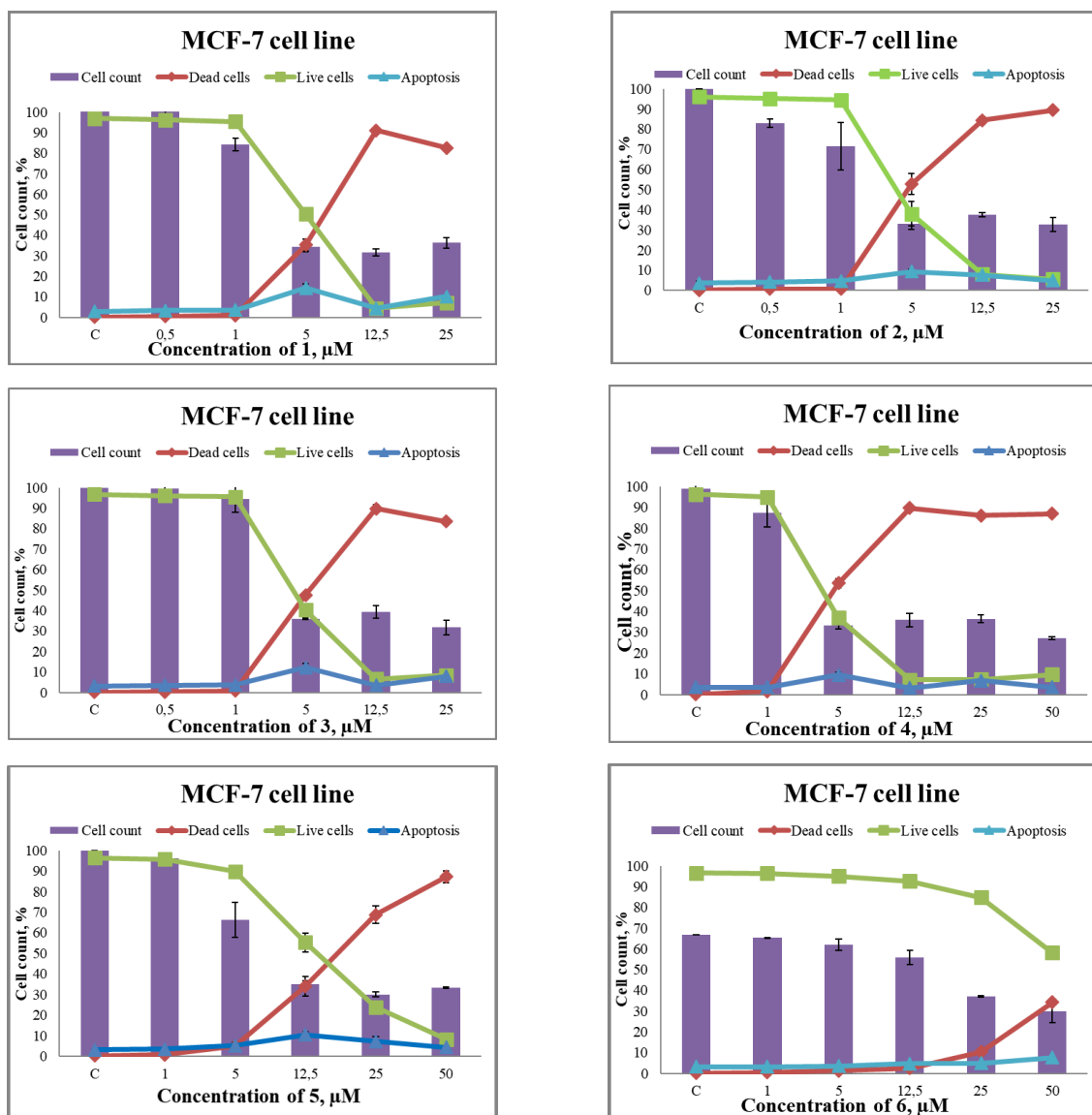


Figure S16. Effect of the copper(II) complexes on the viability of MCF-7 cells determined by dual staining with Hoechst 33342/propidium iodide.

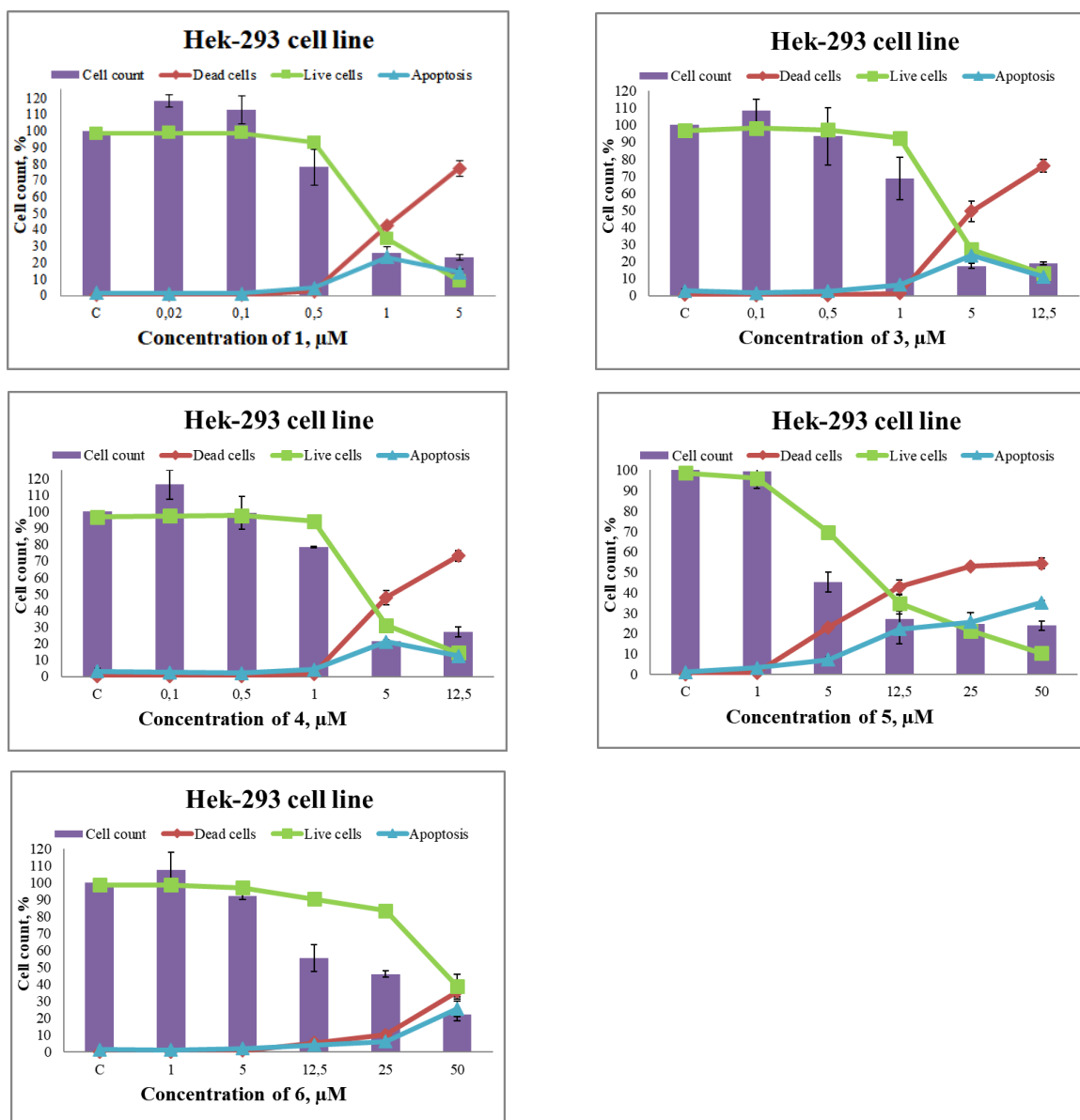


Figure S17. Effect of the copper(II) complexes on the viability of Hek-293 cells determined by dual staining with Hoechst 33342/propidium iodide.

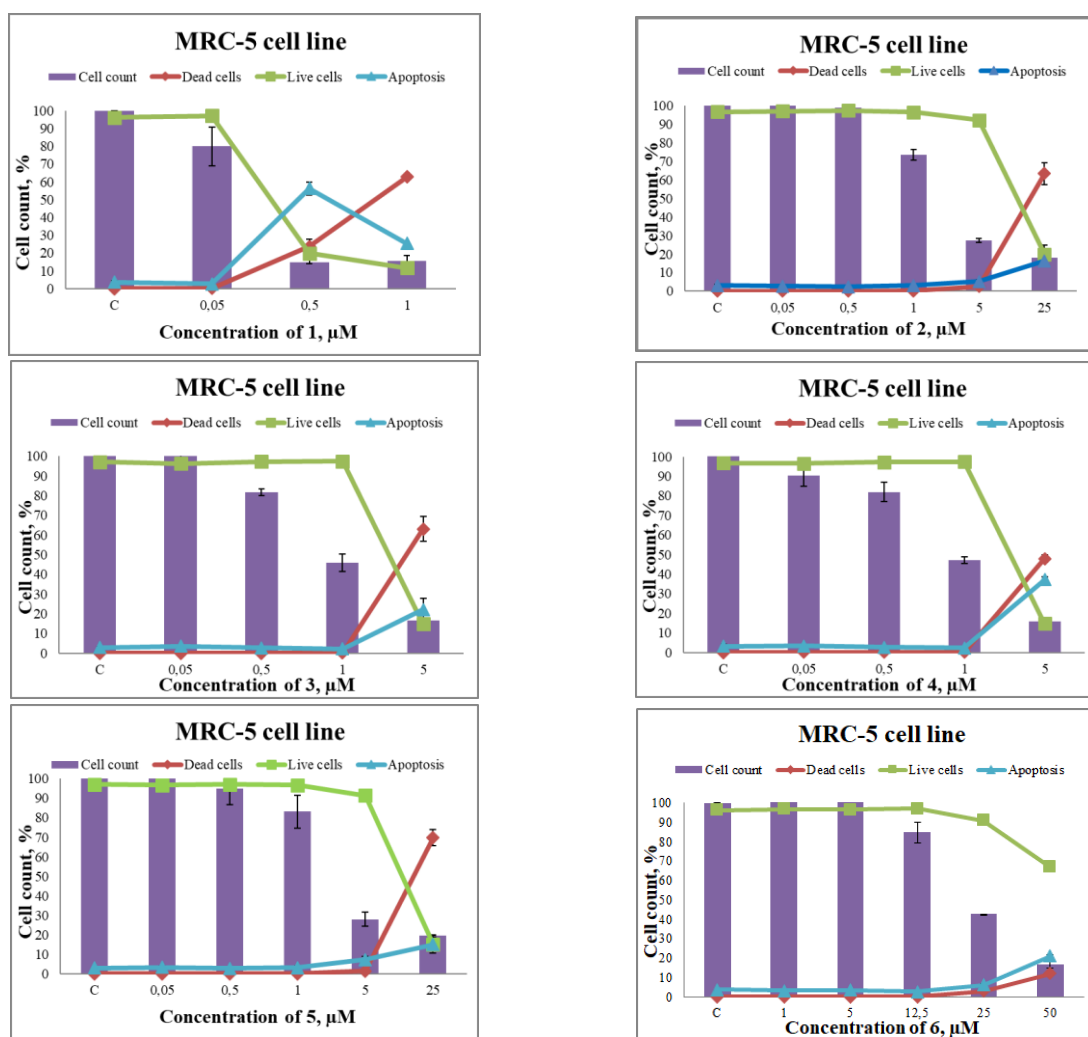


Figure S18. Effect of the copper(II) complexes on the viability of MRC-5 cells determined by dual staining with Hoechst 33342/propidium iodide.